

## THE IDENTIFICATION OF BALMER-DOMINATED FILAMENTS IN RCW 86

KNOX S. LONG<sup>1,2</sup> AND WILLIAM P. BLAIR<sup>1</sup>

Department of Physics and Astronomy, The Johns Hopkins University

Received 1990 March 6; accepted 1990 April 30

### ABSTRACT

We have identified faint optical filaments in the supernova remnant RCW 86 which emit primarily in H $\alpha$  in the wavelength range 6250–7450 Å, unlike the brighter radiative filaments that have been reported previously. The new filaments are similar to the nonradiative filaments seen in other supernova remnants which are thought to arise from fast shock waves interacting with partially neutral interstellar matter. Spectra of these filaments show the H $\alpha$  lines to have two components; the widths of the broad components are consistent with a shock speed in RCW 86 of 500–930 km s<sup>-1</sup>. These shocks have sufficient velocity to produce the X-ray emission observed in RCW 86 and are likely to be associated with the primary blast wave.

*Subject headings:* nebulae: individual (RCW 86) — nebulae: supernova remnants — stars: supernovae — shock waves

### I. INTRODUCTION

In most supernova remnants (SNRs), optical emission is observed from 100–200 km s<sup>-1</sup> shocks traversing dense knots in SN ejecta or the local interstellar medium. The cooling times behind these shocks are short compared to the dynamical time scales of the shocks. As a result, most bright filaments in SNRs have optical spectra in which forbidden lines from a wide range of ionization species including O<sup>0</sup>, O<sup>+</sup>, O<sup>++</sup>, N<sup>+</sup> and S<sup>+</sup> have strengths which are comparable to H $\alpha$  and H $\beta$ . The previously identified filaments in RCW 86 are typical in this regard (Leibowitz and Danziger 1983).

In some SNRs, however, faint filaments exist in which the forbidden lines are very weak or entirely absent. These Balmer-dominated filaments can be understood in terms of a high-velocity shock traversing low-density partially neutral gas (Chevalier and Raymond 1978; McKee and Hollenbach 1980; Chevalier, Kirshner, and Raymond 1980, hereafter CKR). Because the cooling times are long compared to the dynamical time scales for these shocks, they are termed nonradiative. The H $\alpha$  profiles in nonradiative shocks show broad and narrow components; the width of the broad component is directly related to the shock velocity (see, e.g., CKR). Balmer-dominated shocks have been observed previously in SN 1006 (Schweizer and Lasker 1978; Long, Blair, and van den Bergh 1988), Tycho's SNR (Kirshner and Chevalier 1978; Kirshner, Winkler, and Chevalier 1987), Kepler's SNR (Fesen *et al.* 1989), several remnants in the Large Magellanic Cloud (Tuohy *et al.* 1982), and in parts of the Cygnus Loop (Raymond *et al.* 1983; Hester, Raymond, and Danielson 1986). Identification of similar filaments in additional SNRs is important because these filaments are usually associated with the primary shock wave of a SNR which also produces copious X-ray and radio emission.

In this *Letter* we report imaging and spectroscopic observations of RCW 86 which resulted in the discovery of Balmer-dominated filaments in RCW 86. We also give an estimate, based on the H $\alpha$  profile, of the current shock velocity in RCW

86, which is generally (Clark and Stephenson 1977; Strom 1988) though not universally (Huang and Moriarty-Schieven 1987) acknowledged to be the remnant of the historical SN of 185 A.D.

### II. THE OBSERVATIONS AND THEIR REDUCTION

RCW 86 was observed by us as part of an interference filter survey of southern hemisphere SNRs (Blair and Long 1990). The RCW 86 observations were carried out in 1987 April on the 1 m Swope telescope at Las Campanas Observatory in Chile, using a Texas Instruments 800 × 800 pixel CCD with a focal plane reducer, the CHUEI, which compressed the f/7.5 telescope beam down to f/2.7. This instrumental setup produces a relatively large field of 15' with ~1" pixels. The image quality is not ideal, especially at the edges of the field where field curvature and nonuniformities in the CCD degrade the focus. Seeing for our images was ~2", judging from the best star images. Ghost images of bright stars, due to reflections between the interference filters and reimaging optics, are present in some exposures.

Images of two regions of RCW 86 were obtained using the following interference filters: H $\alpha$  ( $\lambda_0 = 6575$  Å, FWHM = 52 Å), [S II] ( $\lambda_0 = 6737$  Å, FWHM = 57 Å), and a red continuum ( $\lambda_0 = 6100$  Å, FWHM = 150 Å). The H $\alpha$  filter is broad enough that [N II]  $\lambda\lambda 6548, 6583$  emission will also be seen in the H $\alpha$  images if it exists. Regions of RCW 86 which were imaged include the bright filaments in the SW portion of the SNR, which had been studied previously by Leibowitz and Danziger (1983), and some filaments on the northern rim of the remnant which are visible on the ESO survey plates but for which no other images or spectra have been published. Typical exposure times ranged from 1000 s for the continuum images to 2000–3000 s for emission-line images. The data were reduced in the following straightforward manner: All of the data were bias-subtracted and flat-fielded with dome flats using IRAF. We then aligned the images using the positions of ~10 stars as fiducials and subtracted the appropriately scaled 6100 Å continuum image from the [S II] and H $\alpha$  images to remove most of the flux from stars (plus sky background and any diffuse continuum which might contaminate the emission-line images). Enlarged portions of the subtracted data for the N and SW fields are shown in Figure 1 (Plate L1) and Figure 2 (Plate L2),

<sup>1</sup> Visiting Astronomer, Las Campanas Observatory, operated by the Carnegie Institution of Washington.

<sup>2</sup> Visiting Adjunct Associate, Mount Wilson and Las Campanas Observatories.

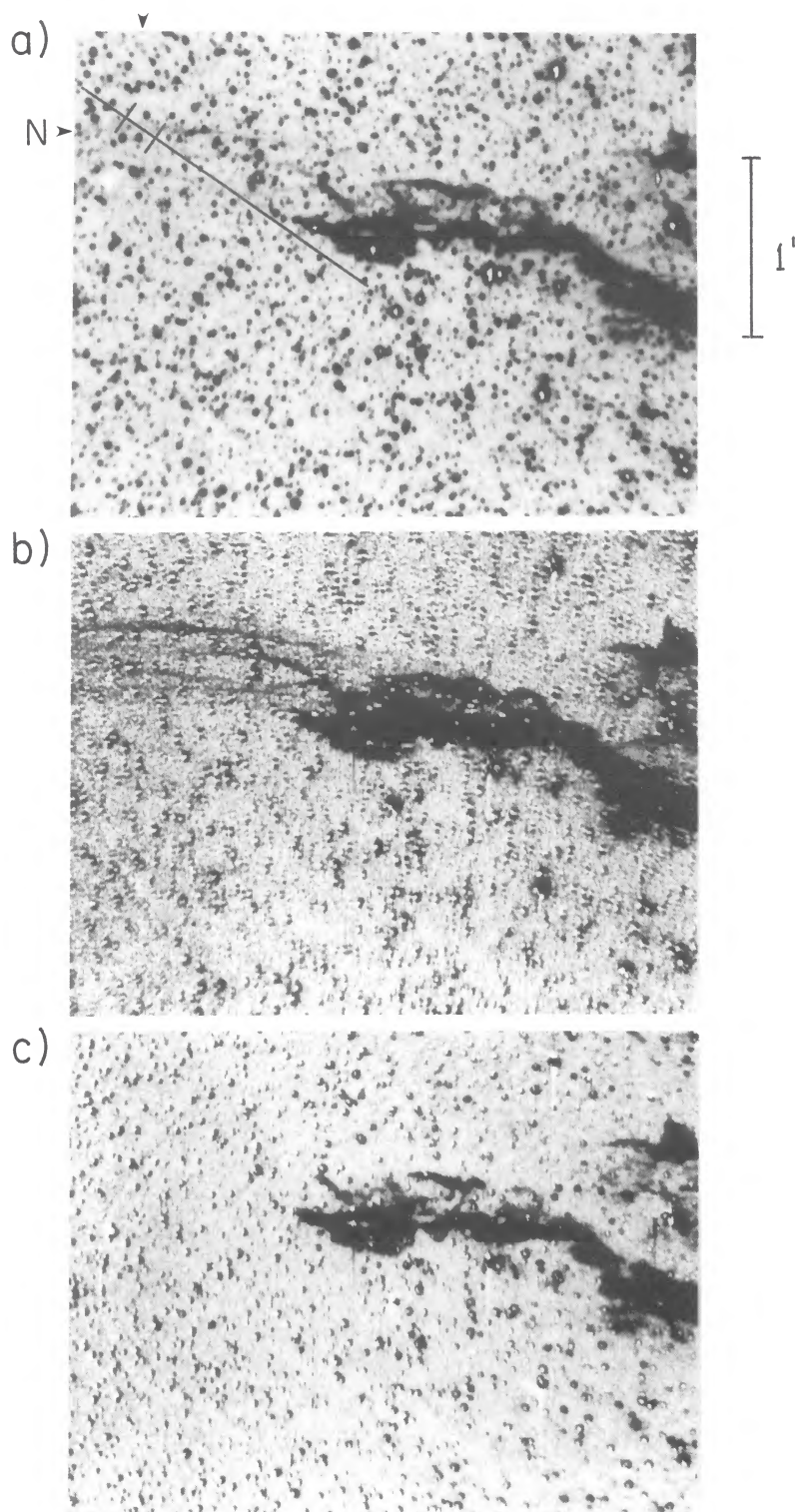


FIG. 1.—A  $2.7 \times 3.5$  section of the northern RCW 86 field. Fig. 1a shows the reduced but unsubtracted H $\alpha$  image. Fig. 1b shows the continuum-subtracted image displayed so that faint emission is emphasized, and Fig. 1c shows the continuum-subtracted [S II] image. The bright filaments in the western half of the images are the radiative filaments which can be seen on the ESO sky survey. The long, wispy filaments in the eastern half of Fig. 1b are not seen in the corresponding [S II] image. The slit positions and the extraction apertures used for the spectroscopic observations are indicated in Fig. 1a.

LONG AND BLAIR (see 358, L13)

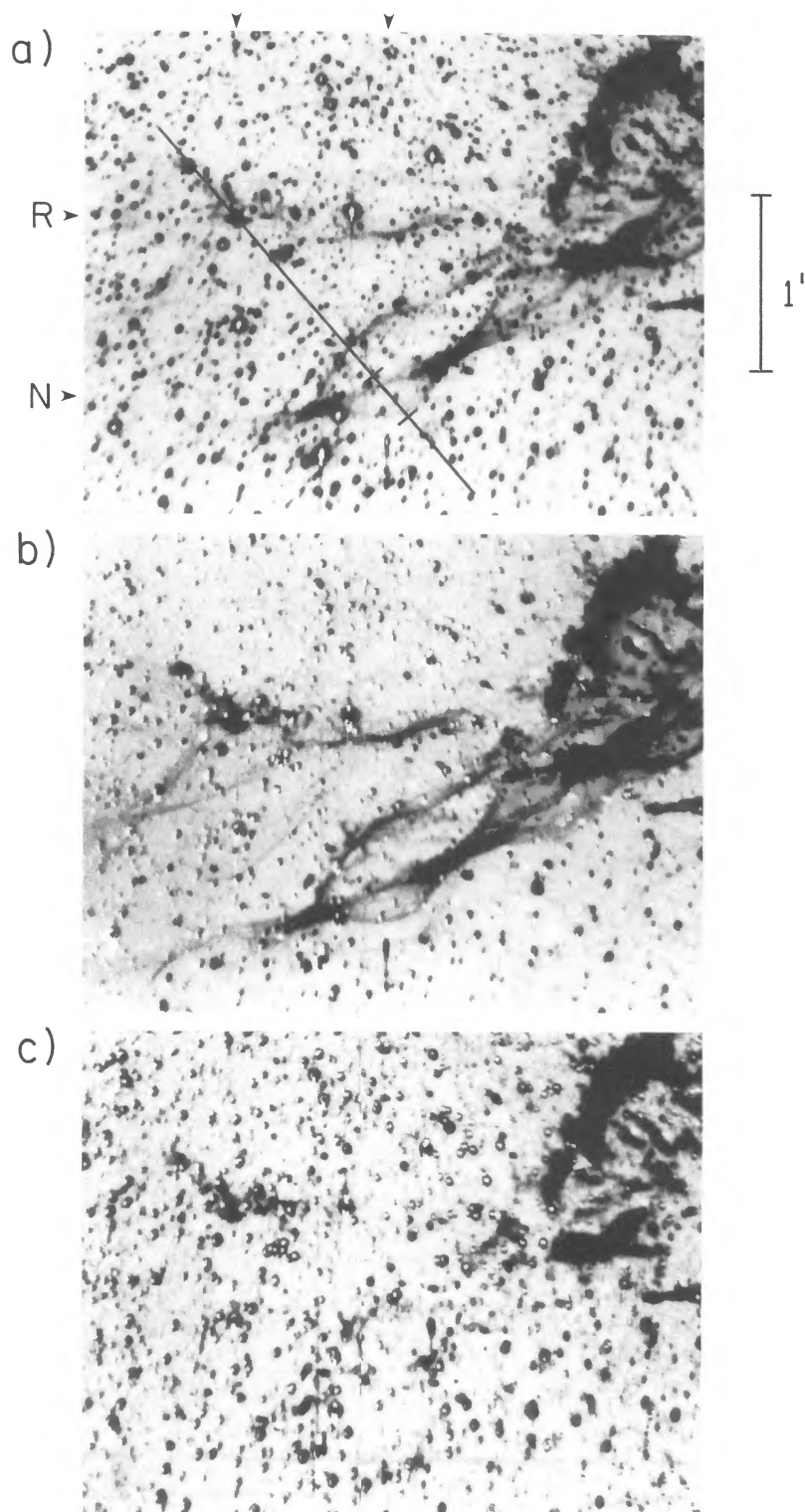


FIG. 2.—A  $2.7 \times 3.5$  section of the southwestern RCW 86 field. Panels are the same as in Fig. 1. The slit position and extraction apertures for the radiative (R) and nonradiative (N) filaments are indicated.

LONG AND BLAIR (*see* 358, L13)

respectively. These figures are centered at  $14^{\text{h}}38^{\text{m}}29^{\text{s}}$ ,  $-62^{\circ}00'05''$  and  $14^{\text{h}}37^{\text{m}}29^{\text{s}}$ ,  $62^{\circ}29'22''$  (1950). The full frame data will be presented in Blair and Long (1990).

Examination of the images revealed not only the bright radiative filaments which have been studied previously and which can be seen in both the [S II] and H $\alpha$  images but also a series of faint lacy filaments visible only in the H $\alpha$  image which extend along the periphery of the SNR in the N and in the SW. The peak surface brightness of these filaments is less than 10% that of the brightest radiative filaments in the images. In both cases H $\alpha$  filaments, which are not visible in the [S II] images, extend east from the bright radiative filaments to the edge of our images. We do not know therefore how far around the periphery of the SNR these filaments extend.

In order to investigate the properties of these filaments further we observed RCW 86 in 1989 February using the

Modular Spectrograph at Las Campanas on the 2.5 m du Pont telescope. The Modular Spectrograph is a long-slit spectrograph which uses a Texas Instruments  $800 \times 800$  CCD as the focal plane detector. For the observations described here we used a  $1200 \text{ line mm}^{-1}$  grating blazed at  $7500 \text{ \AA}$ , a  $2''.5$  slit width, and the 85 mm camera. With this instrumental setup, spectra were obtained covering the wavelength range  $6250\text{--}7450 \text{ \AA}$  with a FWHM resolution of  $\sim 4.1 \text{ \AA}$ . Observations were obtained of the H $\alpha$  filaments both in the N and in the SW with exposure times of 3600 and 5000 s, respectively. In the latter observation the slit also crosses a bright radiative filament in the SW. Slit positions are indicated in Figures 1a and 2a, as are the approximate portions of the slit extracted into one-dimensional spectra in Figure 3. The data from these observations were reduced using IRAF's "Longslit" reduction package; flux calibrations were based on observations of LTT

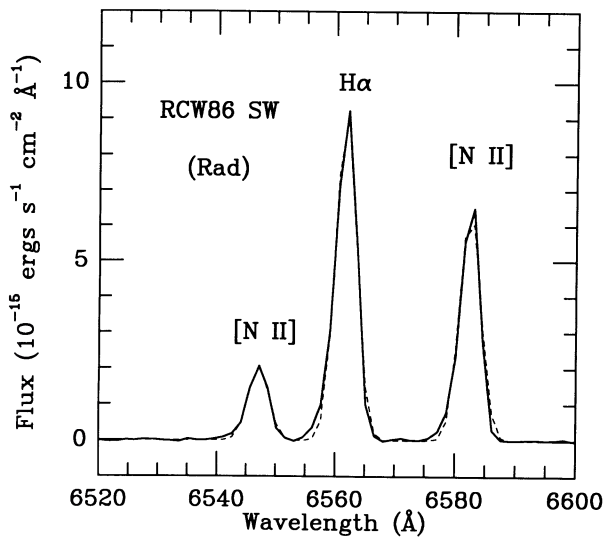


FIG. 3a

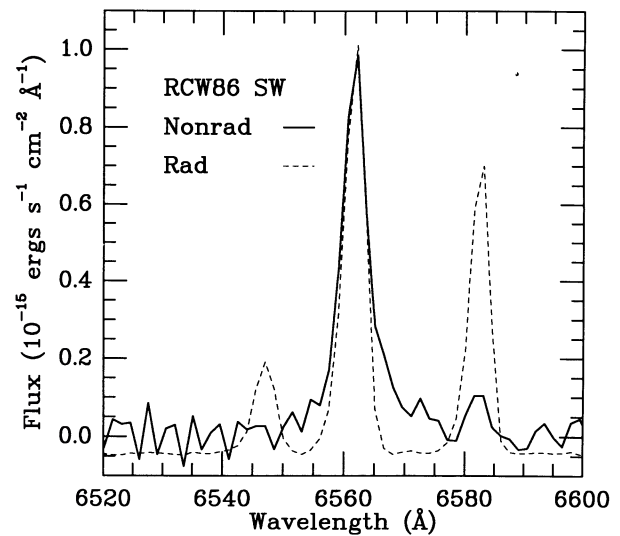


FIG. 3b

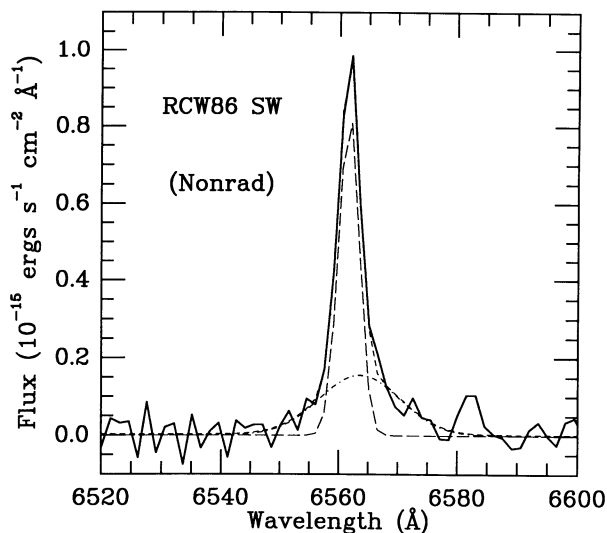


FIG. 3c

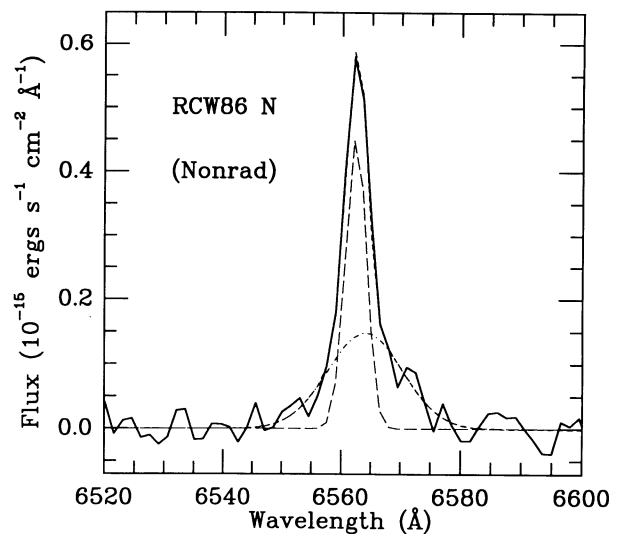


FIG. 3d

FIG. 3.—(a) Portion of the spectrum of a radiative filaments in the SW showing H $\alpha$  and [N II] emission. The dashed line is a Gaussian fit to the data. (b) The same spectral region but for a nonradiative filament in the SW. The dashed line is the spectrum of the radiative filament from (a) rescaled so that the peak of the H $\alpha$  components match. Notice the width of the H $\alpha$  line in the nonradiative filament. (c) The nonradiative filament in the SW fitted with two Gaussians centered near H $\alpha$ . Narrow and broad portions of the H $\alpha$  fit are shown as long-dashed and dot-dashed lines. A short-dashed line (barely visible) shows the overall fit. (d) The nonradiative filament in the north fitted with two Gaussians centered near H $\alpha$ . As before, narrow and broad portions of the H $\alpha$  fit are shown as long-dashed and dot-dashed lines, and the short dashes represent the overall fit.

3864 and LTT 6248 from the list of Stone and Baldwin (1983). Observing conditions were clear but not photometric. We estimate that absolute flux errors are of order 30%, based on intercomparison of the various standard star observations.

Spectra extracted from each slit position confirm that the new filaments are indeed Balmer-dominated, although in a few cases weak [N II] and [S II] emission appears to be present. Figure 3 shows the H $\alpha$  region of a representative set of spectra: (a) a bright radiative filament in the SW, (b) a Balmer-dominated filament in the SW (on which a rescaled spectrum of the radiative filament has been superposed), (c) the same Balmer-dominated filament in the SW (compared to a model fit to the data which is described below), and (d) a Balmer-dominated filament in the N. All of the spectra have been scaled so that the apparent strength of H $\alpha$  is the same. For the radiative filament [N II]  $\lambda$ 6583 is  $\sim \frac{2}{3}$  the strength of H $\alpha$ , whereas in the two Balmer-dominated filaments, [N II]  $\lambda$ 6583 is  $< 10\%$  of H $\alpha$ . In addition, comparison of H $\alpha$  in the three spectra reveals that the profiles in the Balmer-dominated filaments are broader than that of the radiative filament, as expected for nonradiative shock emission.

In order to extract physically meaningful information from the line profiles, we have fitted the H $\alpha$ –[N II] region to a five-component model using a simplex-based line profile fitting code written by G. A. Kriss. The five components comprise a narrow H $\alpha$  line, narrow [N II]  $\lambda$ 6548, 6583, a broad H $\alpha$  line, and a linear background term. The narrow H $\alpha$  and the [N II] lines are all constrained to have the width given by the H $\alpha$  line in a radiative filament. We have also constrained the wavelengths of the [N II] lines relative to narrow H $\alpha$  by performing an initial simplified fit for the wavelength of the narrow H $\alpha$  feature. The position of the broad component of H $\alpha$  is allowed to vary from that of the narrow feature. All of the emission line components are assumed to be Gaussian. The results of the model fits for the spectra are shown in Figures 3a, 3c, and 3d and are listed in Table 1. The FWHM for the broad component in both spectra is  $\sim 15 \pm 2 \text{ \AA}$  ( $1 \sigma$ ). When this is corrected for an instrumental resolution of  $4.1 \text{ \AA}$ , the intrinsic width of the broad component is  $\sim 14.5 \text{ \AA}$  or  $660 \pm 90 \text{ km s}^{-1}$ . The ratio of the broad to narrow component is  $1.0 \pm 0.2 (1 \sigma)$ . In both cases the centroid of the broad line appears shifted to

the red of the narrow feature by  $1.2\text{--}1.4 \text{ \AA}$ , although at the  $3 \sigma$  level the components are coincident.

### III. DISCUSSION

Narrow H $\alpha$  emission arises in collisionless shocks as neutral hydrogen passes through the shock front and is collisionally excited to bound states prior to being ionized by the high-temperature electrons behind the shock. Indeed, each neutral hydrogen atom that enters the shock is expected to produce about 0.2 H $\alpha$  photons (CKR), and as a result in some situations the flux in H $\alpha$  can be used to estimate the density of preshock neutral material. The broad component is produced because some neutrals exchange electrons with fast ions resulting in a population of fast neutrals in the postshock gas which produce Doppler-broadened Balmer emission. According to CKR, both the width of the broad component and the ratio of broad to narrow emission are measures of the shock speed. The exact relationship depends somewhat upon actual conditions in the shock front and the viewing geometry. For CKR's model A, which assumes thermalization of protons only behind the shock, a FWHM of  $660 \pm 90 \text{ km s}^{-1}$  implies a bulk velocity  $v_0$  of material behind the shock of  $\sim 450 \pm 75 \text{ km s}^{-1}$  and a shock velocity ( $v_s = 4/3v_0$ ) of  $600 \pm 100 \text{ km s}^{-1}$ . If H, He, and electrons are thermalized (CKR Model B), the corresponding values are  $v_0 = 600 \pm 100 \text{ km s}^{-1}$  and  $v_s = 800 \pm 130 \text{ km s}^{-1}$ . In this case, the postshock electron temperature would be  $1.3 \pm 0.5 \times 10^7 \text{ K}$ . The H $\alpha$  surface brightness of  $1.2 \times 10^{-6} \text{ ergs cm}^{-2} \text{ s}^{-1} \text{ arcsec}^{-2}$  which we measure for the northern filaments is consistent with a preshock neutral density of  $\sim 0.2 \text{ cm}^{-3}$  for a shock velocity of  $800 \text{ km s}^{-1}$  if the line-of-sight velocity is only  $64 \text{ km s}^{-1}$  as indicated by the separation of  $1.4 \text{ \AA}$  between the centroid of the broad and narrow lines in the north. These estimates are comparable to the X-ray temperature and density deduced for RCW 86 based on a spectral analysis of *Einstein* IPC data (Pisarski, Helfand, and Kahn 1986) and suggest that the Balmer-dominated filaments are closely associated with the X-ray-producing shock in RCW 86.

In principle, the ratio of flux in the broad and narrow emission-line components provides an alternative method for estimating the shock speed. The ratio of broad to narrow line emission in our data— $0.8\text{--}1.2$ —corresponds to values of  $1600\text{--}$

TABLE 1  
SPECTRAL FITS OF H $\alpha$  + [N II] REGION<sup>a</sup>

Spectrum	Line	Flux (ergs cm <sup>-2</sup> s <sup>-1</sup> )	$\lambda$ ( $\text{\AA}$ )	FWHM ( $\text{\AA}$ )
RCW 86 SW (radiative) .....	H $\alpha$ (narrow)	$4.05 \pm 0.05(-14)$	$6561.75 \pm 0.02$	$4.09 \pm 0.05$
	H $\alpha$ (broad)	...	...	...
	[N II] $\lambda$ 6548	$0.92 \pm 0.05(-14)$	$6547.06 \pm 0.11$	$4.18 \pm 0.28$
	[N II] $\lambda$ 6583	$2.72 \pm 0.05(-14)$	$6582.44 \pm 0.07$	$3.78 \pm 0.07$
RCW 86 SW (nonradiative) .....	H $\alpha$ (narrow)	$3.56 \pm 0.20(-15)$	6561.75	4.09
	H $\alpha$ (broad)	$2.80 \pm 0.34(-15)$	$6562.92 \pm 0.75$	$15.03 \pm 2.10$
	[N II] $\lambda$ 6548	$0.03 \pm 0.11(-15)$	6547.06	4.09
	[N II] $\lambda$ 6583	$0.04 \pm 0.11(-15)$	6582.44	4.09
RCW 86 N (nonradiative) .....	H $\alpha$ (narrow)	$2.00 \pm 0.13(-15)$	6562.53	4.09
	H $\alpha$ (broad)	$2.36 \pm 0.21(-15)$	$6563.93 \pm 0.54$	$14.87 \pm 1.54$
	[N II] $\lambda$ 6548	$0.03 \pm 0.07(-15)$	6547.06	4.09
	[N II] $\lambda$ 6583	$0.08 \pm 0.07(-15)$	6582.44	4.09

<sup>a</sup> Errors are  $\pm 1 \sigma$  and represent the statistical uncertainty in the fits; they do not represent the uncertainty in the absolute flux which is  $\pm 30\%$ . Values without errors were fixed prior to fitting. Extraction aperture sizes were 22, 46, and  $34 \text{ arcsec}^2$  for RCW 86 SW (radiative), RCW 86 SW (nonradiative), and RCW 86 N (nonradiative), respectively.

1900 km s<sup>-1</sup> under the assumptions of model A (see, e.g., Fig. 5 of Kirshner, Winkler, and Chevalier 1987). A shock speed of 1800 km s<sup>-1</sup> should produce a broad component with a 40 Å FWHM which is clearly much broader than we observe. Since larger broad to narrow component ratios reduce the estimate of shock velocity, the two estimates might be reconcilable if a modest amount of recombination were enhancing the narrow H $\alpha$  component in these shocks. We note that there is another SNR, 0548–70.4 in the Large Magellanic Cloud, which has a measured broad component similar to RCW 86 ( $760 \pm 160$  km s<sup>-1</sup>; Tuohy *et al.* 1982); in that SNR the ratio of broad to narrow emission is  $1.1 \pm 0.2$  suggesting there is a problem in the interpretation of either the width or the line ratio in this velocity range. As recently discussed by Smith and Kirshner (1989) the problem is most likely in the calculation of the broad to narrow line ratio, which depends sensitively on assumptions about the postshock electron temperature. As a result we regard the width of the broad component as the more reliable estimator of the shock velocity.

The morphology of the H $\alpha$  filaments in RCW 86 differs from the bright radiative filaments as is evident from Figures 1 and 2. The H $\alpha$  filaments in RCW 86 are relatively narrow, gently curved features with gradually changing surface brightness in contrast to the clumpy emission observed from the bright filaments known previously. This suggests that the H $\alpha$  filaments probe a large filling factor portion of the ISM surrounding RCW 86. It appears likely that the emission is arising from sheets of material whose thickness is much less than the characteristic length scale. Especially in the north, the sheets appear to lie preferentially along the outside edge of the SNR. In this regard, the morphology of the new filaments in RCW 86 resembles that of the Balmer-dominated filaments which have been observed in Tycho's SNR (Kirshner, Winkler, and Chevalier 1987), SN 1006 (Long, Blair, and van den Bergh 1988), and the Cygnus Loop (Raymond *et al.* 1983).

RCW 86 is a shell-like X-ray and radio source with a diameter of  $\sim 45'$ . The Balmer-dominated filaments we have observed are located within the X-ray shell of RCW 86 (Pisarski, Helfand, and Kahn 1984) and lie along the outer edges of radio filaments in Milne *et al.*'s (1985) radio map. Estimates of the distance to RCW 86 have ranged recently from  $\sim 1$  kpc to 3.2 kpc with more recent estimates tending toward lower values (Green 1984; Strom 1988). If RCW 86 is the remnant of SN 185 A.D. and if it evolved from the free expansion phase to the Sedov phase early in its history, then the shock speed  $v_s$  of RCW 86 today would be given by

$$v_s = \frac{2}{3} \langle v \rangle = 1480 D_{\text{kpc}} \text{ km s}^{-1},$$

where  $D_{\text{kpc}}$  is the distance in kpc and  $\langle v \rangle$  is the mean expansion velocity. If the filaments we observe are due to the primary shock wave in RCW 86 our spectra of Balmer line filaments clearly argue for a distance of  $\leq 1$  kpc as do most estimates based on the identification of RCW 86 with SN 185 A.D. Even if this is not the case, the distance to RCW 86 can be established directly when the proper motion of the Balmer filaments is measured accurately. This proper motion should be  $\sim 0''.17$  yr<sup>-1</sup> for  $D_{\text{kpc}} = 1$  and  $v_s = 800$  km s<sup>-1</sup>. An accurate determination of the distance is clearly important given the questions posed by Huang and Moriarty-Schieven's (1987) reinterpretation of the Chinese record on SN 185 A.D.

We wish to thank the Observatories of the Carnegie Institution of Washington for the use and support of the telescopes and instrumentation necessary to carry out these observations. We would also like to thank G. A. Kriss whose excellent line-fitting program saved us a great deal of time and effort and R. P. Kirshner who provided the interference filters. David Handwerker assisted in the image reductions. This work was supported by the Center for Astrophysical Sciences of the Johns Hopkins University.

#### REFERENCES

- Blair, W. P., and Long, K. S. 1990, in preparation.  
 Chevalier, R. A., Kirshner, R. P., and Raymond, J. C. 1980, *Ap. J.*, **235**, 186 (CKR).  
 Chevalier, R. A., and Raymond, J. C. 1978, *Ap. J. (Letters)*, **225**, L27.  
 Clark, D. H., and Stephenson, F. R. 1977, *The Historical Supernovae* (Elmsford, N.Y.: Pergamon), p. 83.  
 Fesen, R. A., Becker, R. H., Blair, W. P., and Long, K. S. 1989, *Ap. J. (Letters)*, **338**, L13.  
 Green, D. A. 1984, *M.N.R.A.S.*, **209**, 449.  
 Hester, J. J., Raymond, J. C., and Danielson, G. A. 1986, *Ap. J. (Letters)*, **303**, L17.  
 Huang, Y.-L., and Moriarty-Schieven, G. H. 1987, *Science*, **235**, 59.  
 Kirshner, R. P., and Chevalier, R. A. 1978, *Astr. Ap.*, **67**, 267.  
 Kirshner, R. P., Winkler, P. F., and Chevalier, R. A. 1987, *Ap. J. (Letters)*, **315**, L35.  
 Leibowitz, E. M., and Danziger, I. J. 1983, *M.N.R.A.S.*, **204**, 273.  
 Long, K. S., Blair, W. P., and van den Bergh, S. 1988, *Ap. J.*, **333**, 749.  
 McKee, C. F., and Hollenbach, D. J. 1980, *Ann. Rev. Astr. Ap.*, **18**, 219.  
 Milne, D. K., Caswell, J. L., Haynes, R. F., Kesteven, H. J., Roger, R. S., and Bunton, J. D. 1985, *Proc. Astr. Soc. Australia*, **6**, 78.  
 Pisarski, R. L., Helfand, D. J., and Kahn, S. M. 1984, *Ap. J.*, **277**, 710.  
 Raymond, J. C., Blair, W. P., Fesen, R. A., and Gull, T. R. 1983, *Ap. J.*, **275**, 636.  
 Schweizer, F., and Lasker, B. M. 1978, *Ap. J.*, **226**, 167.  
 Smith, R. C., and Kirshner, R. P. 1989, *Bull. AAS*, **21**, 1201.  
 Stone, R. P. S., and Baldwin, J. A. 1983, *M.N.R.A.S.*, **204**, 347.  
 Strom, R. G. 1988, *M.N.R.A.S.*, **230**, 231.  
 Tuohy, I. R., Dopita, M. A., Mathewson, D. S., Long, K. S., and Helfand, D. J. 1982, *Ap. J.*, **261**, 473.

WILLIAM P. BLAIR and KNOX S. LONG: Center for Astrophysical Sciences, The Johns Hopkins University, Charles and 34th Streets, Baltimore, MD 21218